Zeolitic Imidazolate Frameworks for Kinetic Separation of Propane and Propene

Kunhao Li,[†] David H. Olson,[†] Jonathan Seidel,[†] Thomas J. Emge,[†] Hongwei Gong,[‡] Heping Zeng,[‡] and Jing Li*,[†,‡]

Department of Chemistry and Chemical Biology, Rutger, The State University of New Jersey, 610 Taylor Road, Piscataway, New Jersey 08852, and College of Chemistry, South China University of Technology, Guangzhou, 510006, P. R. China

Received May 21, 2009; E-mail: jingli@rutgers.edu

Industrial olefin/paraffin separations heavily rely upon energy-intensive distillation-based technologies, which represent a class of the most important and also the most costly processes in the chemical industry.[1] Adsorptive separation is widely considered as a more energy and cost-efficient alternative. The structures and properties of the adsorbent materials often dictate the separation mechanisms that apply: molecular sieving or steric size exclusion, equilibrium or kinetics based separation.[2] While most adsorbents (exclusively zeolites or amorphous adsorbents) studied for olefin/paraffin separations achieve such separations by their preferential equilibrated uptake of one component versus the other or by size exclusion, there are a limited number of cases where the separations are accomplished by differences in the diffusion rates of the adsorbates (olefin and paraffin) into and out of the adsorbents.[2,3] Microporous metal organic frameworks (MMOFs), as a new type of crystalline adsorbent materials, have shown great potential in hydrocarbon separations.[4] Very recently, the possibility of equilibrium-based olefin/paraffin separations by MOFs was investigated.[5] Herein, we report the first examples of MMOFs that are capable of kinetic separation of propane and propene (propylene), which is one of the most difficult chemical separations due to their very close relative volatilities and molecular sizes.

The MMOFs we studied belong to a recently emerged group of materials named Zeolitic Imidazolate Frameworks (ZIFs).[5] Their structures are constructed upon metals of tetrahedral coordination geometry (e.g, Zn[II] and Co[II]) and imidazole ligands (e.g., 2-chloroimidazole (2-cim) for **1** and 2-bromoimidazole (2-bim) for **2** herein), which closely resemble the structures of zeolites. In addition to their excellent thermal and chemical stability, they also lack Lewis and Brønsted acid sites that may catalyze polymerization of olefins inside the pores. For zeolites, only those with high silica content can be used for separation of olefin/paraffin whereas their synthesis can be difficult.

Reacting $Zn(NO_3)_2 \cdot 6H_2O$ with 2-cim and 2-bim in methanol under solvothermal conditions resulted in good quality polyhedral crystals of $[Zn(2\text{-cim})_2] \cdot 2.1(CH_3OH)$ (**1**) and $[Zn(2\text{-bim})_2] \cdot 0.16(H_2O) \cdot 0.16(C_2H_5OH)$ (**2**), respectively (see Supporting Information). Single crystal X-ray diffraction revealed that **1** and **2** are iso-structural to each other, both crystallizing in the cubic $I\bar{4}3m$ space group with almost identical unit cell constants (Supporting Information). Zn[II] centers are invariably tetrahedrally coordinated to four N atoms from four imidazolate ligands. Each imidazole coordinates to two Zn[II] with Zn−Im−Zn angles (θ, Figure 1d) close to 145°, which are coincident with the typical Si−O−Si angles found in many zeolites. This has been reasonably attributed to be the main structural directing factor in the formation of zeolite-like frameworks.[6] In this case, both **1** and **2** have an expanded sodalite (*sod*)[7] framework structure (Figure 1a). The square faces of the truncated octahedral cages are essentially blocked by the chlorine or bromine atoms (Figure 1b); therefore, the cages are interconnected along 3-fold axes through the small openings delimited by H atoms on imidazolate ligands (Figure 1c).
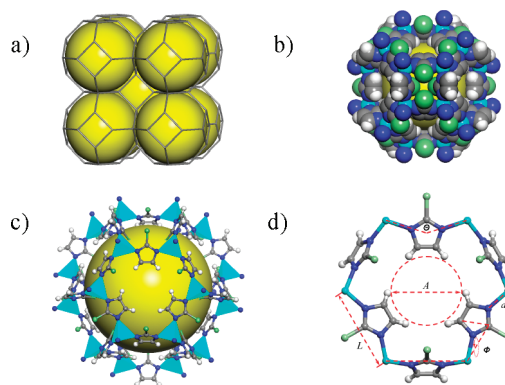
Figure 1. (a) Expanded sodalite (*sod*) framework formed by connecting the tetrahedral Zn[II] centers; (b) space-filling model of one *sod* cage; (c) view of the pore opening along one 3-fold axis; (d) labeling scheme of the structural features determining the pore opening size. C: gray; H: white; N: blue; Zn: light blue; Cl or Br (or methyl in **3**): light green. All disordered solvent molecules were removed for clarity. Yellow spheres indicate the cavity inside the cages ($\sim$12.5 Å in diameter).

Compound **1** and **2** are isostructural to the recently reported ZIF-8 structure (**3**, with 2-methylimidazole as the ligand, Supporting Information).[6] Considering the comparable sizes of chloro, bromo, and methyl groups, the similarity in their overall structure is expected. However, the slight differences in the sizes of the three substituents (and possibly in combination with their different electronic inductive effects) lead to small but significant perturbations to the Zn−N bond distances (d), Zn−Im−Zn angles (θ) and the dihedral angles between the imidazole ring and the hexagonal faces enclosed by 6 Zn[II] centers (Φ), and Zn−Zn distances (L), which result in different effective pore opening (aperture) sizes (A, Figure 1d and Table 1). It is shown in the following study that the seemingly small differences in their effective pore opening sizes (<0.2 Å) are actually critical to their propane/propylene ($C_3^\circ/C_3^=$) separation capabilities.

Under equilibrium conditions, propane and propene adsorption measurements on **3** revealed essentially identical adsorption capacities for both, 155 and 160 mg/g at 30 °C and 600 Torr. In addition, their isosteric heats of adsorption at zero loading are similar, 34 and 30 kJ/mol, respectively (Supporting Information). While

† The State University of New Jersey.
‡ South China University of Technology.

Table 1. Structural Factors Determining the Effective Size of the Pore Openings, A (Excluding van der Waals Radius of H)

	θ (deg)	d (Å)	Φ (deg)	L (Å)	A (Å)
1	142.62	1.983	5.328	6.004	3.37
2	144.35	1.995	7.032	6.032	3.54
3	144.77	1.984	10.764	6.015	3.26

thermodynamic separation seems impractical, the rates of adsorption are markedly different (Figure 2). At 30 °C, the ratio of their diffusion rate coefficients, $D(C_3^\circ)/D(C_3^=)$, is 125, suggesting that **3** has great potential for the kinetic separation of these two very similar molecules. Adsorption rate measurements for **1** have also yielded the relative adsorption rates of propene and propane. At 30 °C the ratio of their diffusion rates is 60, approximately one-half that of **3** (Figure 2).
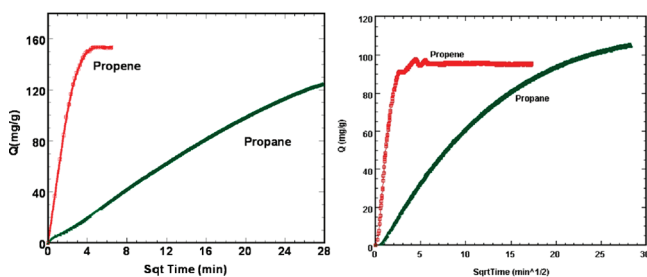
Figure 2. Propene and propane uptake by **3** (left) and **1** (right) as a function of square root of time.

As found for a few eight-membered ring zeolites, separation of light hydrocarbons such as propane and propene is controlled by the critically sized pore openings.[8] In spite of the minimal size differences of propane and propene of no more than 0.2 to 0.3 Å,[9] the energy barriers for the two molecules passing through the pore openings can be very different. The activation energies found for propene and propane are 9.7 and 74.1 kJ/mol, respectively, within **1**. The lower discrimination by **1** (compared to **3**) suggests that the propane/propene separation capability is very sensitive to the effective sizes of the pore openings. Accordingly, **2** is expected to have an even lower ratio of the diffusion rate coefficients of propene/propane due to its even larger pore opening. It shall also be noted that although the propene (and propane) uptake rate found for this particular preparation of **3** (with crystal size ~150 μm, Supporting Information) is not yet reaching an optimum for an efficient kinetics-based pressure swing adsorption (PSA) separation process, smaller crystals can be easily made for faster pressure swing cycles.

In summary, the single-component diffusion rate study reveals that kinetic separation of propane/propene by a series of metal−imidazolate zeolitic framework materials is highly probable based on the remarkable differences in their diffusion rates through the pore systems. The effective size of the pore opening is believed to be the controlling factor determining the separation capability. In-depth studies to assess the full separation capability of these materials, e.g., the breakthrough performance, process efficiency, and cost simulations, etc., are currently underway.

Supporting Information Available: Syntheses of 2-cim; crystal growths and selected crystallographic data of **1**, **2**, and **3**; adsorption measurement procedures and additional figures. These materials are available free of charge via the Internet at http://pubs.acs.org.

References

(1) Eldridge, R. B. *Ind. Eng. Chem. Res.* **1993**, *32* (10), 2208–2212.
(2) Yang, R. T. *Gas Separation by Adsorption Processes*; Imperial College Press: 1997.
(3) Padin, J.; Rege, S. U.; Yang, R. T.; Cheng, L. S. *Chem. Eng. Sci.* **2000**, *55* (20), 4525–4535. Jarvelin, H.; Fair, J. R. *Ind. Eng. Chem. Res.* **1993**, *32* (10), 2201–2207.
(4) Snurr, R. Q.; Hupp, J. T.; Nguyen, S. T. *AIChE J.* **2004**, *50* (6), 1090–1095. Li, J.-R.; Kuppler, R. J.; Zhou, H.-C. *Chem. Soc. Rev.* **2009**, *38* (5), 1477–1504. Czaja, A. U.; Trukhan, N.; Mueller, U. *Chem. Soc. Rev.* **2009**, *38* (5), 1284–1293. Dubbeldam, D.; Galvin, C. J.; Walton, K. S.; Ellis, D. E.; Snurr, R. Q. *J. Am. Chem. Soc.* **2008**, *130*, 10884–10885. Barcia, P. S.; Zapata, F.; Silva, J. A.; Rodrigues, A. E.; Chen, B. *J. Phys. Chem. B* **2007**, *111*, 6101–6103. Pan, L.; Parker, B.; Huang, X. Y.; Olson, D. H.; Lee, J.; Li, J. *J. Am. Chem. Soc.* **2006**, *128* (13), 4180–4181. Pan, L.; Olson, D. H.; Ciemnolonski, L. R.; Heddy, R.; Li, J. *Angew. Chem., Int. Ed.* **2006**, *45* (4), 616–619. Li, K.; Olson, D. H.; Lee, J.; Bi, W.; Wu, K.; Yuen, T.; Xu, Q.; Li, J. *Adv. Funct. Mater.* **2008**, *18*, 2205–2214. Li, K. H.; Lee, J.; Olson, D. H.; Emge, T. J.; Bi, W. H.; Eibling, M. J.; Li, J. *Chem. Commun.* **2008**, (46), 6123–6125. Ma, S. Q.; Sun, D. F.; Wang, X. S.; Zhou, H. C. *Angew. Chem., Int. Ed.* **2007**, *46* (14), 2458–2462. Chen, B. L.; Liang, C. D.; Yang, J.; Contreras, D. S.; Clancy, Y. L.; Lobkovsky, E. B.; Yaghi, O. M.; Dai, S. *Angew. Chem., Int. Ed.* **2006**, *45* (9), 1390–1393. Hartmann, M.; Kunz, S.; Himsl, D.; Tangermann, O.; Ernst, S.; Wagener, A. *Langmuir* **2008**, *24* (16), 8634–8642.
(5) Lamia, N.; Jorge, M.; Granato, M. A.; Almeida, F. A.; Chereau, H.; Rodrigues, A. E. *Chem. Eng. Sci.* **2009**, *64*, 3246–3259. Alaerts, L.; Maes, M.; Van der Veen, M.; Jacobs, P.; De Vos, D. E. *Phys. Chem. Chem. Phys.* **2009**, *11*, 2903–2911. Hartmann, M.; Kunz, S.; Himsl, D.; Tangermann, O.; Ernst, S.; Wagener, A. *Langmuir* **2008**, *24*, 8634–8642.
(6) Park, K. S.; Ni, Z.; Cote, A. P.; Choi, J. Y.; Huang, R. D.; Uribe-Romo, F. J.; Chae, H. K.; O'Keeffe, M.; Yaghi, O. M. *Proc. Natl. Acad. Sci. U.S.A.* **2006**, *103* (27), 10186–10191. Huang, X. C.; Lin, Y. Y.; Zhang, J. P.; Chen, X. M. *Angew. Chem., Int. Ed.* **2006**, *45* (10), 1557–1559.
(7) Reticular Chemistry Structure Resource. http://rcsr.anu.edu.au.
(8) Ruthven, D. M.; Reyes, S. *Microporous Mesoporous Mater.* **2007**, *104*, 59–66. Hedin, N.; DeMartin, G. J.; Roth, W. J.; Strohmaier, K. G.; Reyes, S. C. *Miroporous Mesoporous Mater.* **2008**, *115*, 585–593. Barrett, P. A.; Boix, T.; Puche, M.; Olson, D. H.; Jordan, E.; Koller, H.; Camblor, M. A. *Chem. Commun.* **2003**, (17), 2114–2115. Olson, D. H.; Camblor, M. A.; Villaescusa, L. A.; Kuehl, G. H. *Microporous Mesoporous Mater.* **2004**, *67* (1), 27–33. ter Horst, J. H.; Bromley, S. T.; van Rosmalen, G. M.; Jansen, J. C. *Microporous Mesoporous Mater.* **2002**, *53* (1−3), 45–57.
(9) Zhu, W.; Kapteijn, F.; Moulijn, J. A. *Chem. Commun.* **1999**, (24), 2453–2454.

JA9039983